

ELECTROCHEMICAL REACTIVITY AND WETTING PROPERTIES OF ANODES MADE FROM ANISOTROPIC AND ISOTROPIC COKES

Camilla Sommerseth¹, Rebecca Jayne Thorne¹, Arne Petter Ratvik², Espen Sandnes¹, Stein Rørvik², Lorentz Petter Lossius³, Hogne Linga³ and Ann Mari Svensson¹

¹Dept. of Materials Science and Engineering, Norwegian University of Science and Technology, NO-7491 Trondheim, Norway

²SINTEF Materials and Chemistry, NO-7465 Trondheim, Norway

³Hydro Aluminium AS, Ardal, Norway

Keywords: Carbon Anodes, Anisotropic Coke, Isotropic Coke, Electrochemical Reactivity, Wetting Properties

Abstract

As the quality of the coke available for production of anodes is deteriorating, future production will rely on cokes that are more isotropic with higher impurity levels than traditional raw materials. The purpose of this work was to improve the understanding of the electrochemical reactivity and wetting properties in relation to the type of coke. Anode:electrolyte wetting is a key factor towards determining electrochemical reactivity, which in turn is affected by anode properties and polarization. Pilot anodes were fabricated from single source cokes; one anisotropic coke low in impurities, and one isotropic coke with significantly higher impurity levels. Electrochemical characterisation included chronopotentiometry, cyclic voltammetry and impedance spectroscopy. Wetting properties were studied on both unpolarised and polarised samples by a dedicated wetting apparatus, and indirectly by computed tomography (CT) images of frozen electrolyte films.

Introduction

The quality of anode grade coke has changed the past decade due to shortage in supplies of traditional anisotropic sponge coke, and coke that was previously rejected by the aluminium industry, are now being blended into the coke aggregate by many carbon anode producers [1], [2].

An improved knowledge on how isotropic cokes influence the electrochemical behaviour of anodes is needed and has been investigated to some extent in [3], [4], [5]. The overpotential is a source of increased energy consumption. Equation 1 summarises the measured anodic potential, where E^{rev} is the reversible potential (1.187 V w.r.t. Al/Al³⁺ [6]), η_c is the con-

centration overpotential at the anode surface, and in a saturated melt this overpotential may be considered negligible. η_r^0 is the reaction overpotential and this will vary with anode material when using the vertical anode setup as described in [4]. η_h is overpotential caused by hyperpolarisation due to bubbles on the surface. The last term in Equation 1 is describing the increased ohmic resistance at the anode caused by bubble build-up: δR_s denotes the ohmic resistance due to bubbles blocking the anode surface and R'_s is the ohmic resistance at the surface with not bubbles screening the anode. Due to the vertical anode setup used, η_h , δR_s and R'_s are negligible. Thorne et al. found that a slight reduction in reaction overpotential could be found when using isotropic coke compared to anisotropic sponge coke in anodes [4].

$$E_{\text{measured}} = E^{\text{rev}} + \eta_c + \eta_r^0 + \eta_h + I(R'_s + \delta R_s) \quad (1)$$

Electrical impedance spectroscopy can be used in order to investigate the electrochemical reactivity of anodes [7], where the capacitance of the anode surface is attributed to how well wetted the anode surface is by electrolyte [8]. An increase in capacitance of about 45 % was seen on a polarised anode sample compared with a fresh anode sample, and this capacitance increase was attributed to higher surface area exposed to electrolyte. Thonstad [7] measured a double layer capacitance range for pyrolytic graphite between 45-75 $\mu\text{F}/\text{cm}^2$ and a range for baked carbon between 150-600 $\mu\text{F}/\text{cm}^2$ using a horizontal anode setup. In this work, capacitance is used in order to determine the charge per anode area for the different anode materials used. Thorne et al. [4] found a slight increase in capacitance when analysing an isotropic coke anode compared with an anisotropic coke anode, denoted as Anode 1 and Anode 4, respectively.

The anode:electrolyte interaction is another important

feature when producing aluminium, and the wetting properties of the anode surface towards the electrolyte is important. Some trends have been found in terms of electrolyte composition and polarised samples vs. unpolarised samples. These trends are summarised in [6] and [9]. Solheim et al. [9] described how wetting properties change after polarisation of an anode surface compared with an unpolarised surface. It was especially the receding wetting angle that changed when an anode was lifted out of a cryolitic electrolyte before and after polarisation. CT imaging can also be used to investigate the frozen electrolyte image on an anode sample and is hence anticipated to reflect the wetting properties on the anode:electrolyte interface [10]. The sessile drop method was used in order to investigate the anode:electrolyte on an unpolarised surface by Thorne et al. [5]. It was found that for both graphite and the anisotropic coke materials, the anode:electrolyte wetting angles were of non-wetting character, i.e. $\theta > 90^\circ$. The isotropic anode materials showed a wetted character between anode:electrolyte, i.e. $\theta < 90^\circ$. The sessile drop method is an equilibrium measurement, where a very small electrolyte sample is placed on the anode surface. There are some sources of error with this method, including the small electrolyte sample on the very small anode surface area, the fact that the electrolyte:anode interface is stagnant and that no polarisation is applied. The literature has often described the effect of polarisation on the wetting conditions between electrolyte and anode in e.g. [6], [9].

In this work, the electrochemical reactivity of anodes towards a cryolitic electrolyte was investigated through overpotential measurements and capacitance measurements using electrical impedance spectroscopy. The wetting properties of the anode toward the electrolyte was investigated using two different methods: 1) a dedicated wetting apparatus where the effect of polarisation was investigated, as explained in [9], [11] and 2) by CT imaging investigating the effect of the bathfilm thickness when pulling the anode out of the electrolyte with and without current on. Methodology of CT imaging is thoroughly described in [10] and will not be described further here.

Experimental

Pilot anodes ($\varnothing = 130$ mm, $h = 180$ mm) were specially designed and made at Hydro Ardalstangen for this experimental work. The anodes were produced from single source industrial grade cokes, one

of anisotropic character: Anode A, and the other of purely isotropic character: Anode B. The same industrial grade pitch was used for both pilot anodes. <2 mm coke aggregate were produced to a common sieve curve from ball milled coke (fines $<63\mu\text{m}$), 0-1 mm and 1-2 mm fractions. Fractions of <2 mm coke particles were chosen in order to maintain a representative exposed surface area during small scale electrochemical tests. In this work, two different anode materials were studied; for clarity, Anodes A and B in this work are identical to Anode A and B in Sommerseth et al. [10], also Anode A = Anode 1 and Anode B = Anode 4 in [3], [4] and [5], however, new parallels samples have been made for all electrochemical tests. Ultra-pure graphite (CMG grade) from Svensk Specialgrafit AB was used as reference material.

During electrochemical tests an experimental setup and anode assembly similar to that described in Figure 1 by Thorne et al. [3] was used. The vertical anode assembly gave a well-defined, starting geometrical surface area of 1.52 cm^2 and negligible bubble noise. The surface area was not corrected for due to consumption of the anodes, however, the electrolysis time was kept to a minimum in order to change the geometrical anode surface area as little as possible. The electrolyte was a cryolite melt with a $\text{NaF}:\text{AlF}_3$ molar ratio of 2.3, corresponding to 9.8 wt% excess of aluminium fluoride, AlF_3 . The cryolite was from Sigma-Aldrich ($>97\%$) and the AlF_3 was sublimed in-house for purification. The electrolyte was saturated in $\gamma\text{-Al}_2\text{O}_3$ (9.4 wt%) from Merck.

Electrochemical reactivity of anode A and B was tested by slow sweep-rate cyclic voltammetry (CV) at 0.1 V/s from open circuit potential (OCP) to 2.5 V, chronopotentiometry (CP) at 1.0 A/cm^2 and capacitance measurements through electrical impedance spectroscopy (EIS) at 1.5 V (non-IR corrected). The slow sweep rate CV's gave similar results to steady-state polarisation curves [4]. Measurements were performed using a Zahner IM6 with built in EIS module and 20 A booster (PP201, from Zahner-Elektrok). Ohmic resistance was determined by taking the high frequency Z_{Re} intercept from the Nyquist plot obtained by EIS at OCP and this resistance was used to IR correct all electrochemical tests. An aluminium reference electrode was used. A new Al reference electrode was produced per duplicate run. Capacitance was extracted from Nyquist plots (EIS at 1.5 V) by three different methods: 1) modelling by the equivalent circuit LR(CR) and extracting the double layer

capacitance (C_{dl}) directly, 2) modelling by the equivalent circuit LR(Q(R(LR))) and calculating the effective capacitance from Q according to Equation 13.10 in [12] and 3) extracting C_{dl} directly by extracting the inductance directly at the highest frequency (100 000 Hz) and using the high frequency range of the Nyquist plot to determine the capacitance as described in [8].

Rod shaped anodes ($\varnothing = 9.7$ mm, $h = 5$ mm) were polarised for 1500 s at 1.0 A/cm² and electrolyte removed by soaking in saturated AlCl₃ solution until all remaining electrolyte on the surface was removed. The horizontal surface area was then investigated in a confocal microscope (Infinitefocus from Alicona 3D) in order to determine the surface roughness of the anode surface after polarisation. The software for the microscope then calculated true area (including all voids and pores) over projected (geometrical) area of the horizontal surface area. This true area over projected area was then used to normalise the capacitance for true surface area including all voids and pores.

The “dynamic” wetting angle for the anode:electrolyte interface was determined before and after polarisation at 0.7 A/cm² for 10 s, using the method described in [9] and [11]. This experimental setup was used with a slight modification: the anode cup samples in this work had an outer diameter of 30 mm and an inner diameter of 22 mm. The wetting angle reported here are during immersion of the anode sample into the electrolyte due to more noisy recordings during the emersion of the sample.

The wetting properties of the anode:electrolyte interface for the two different anode samples were also investigated using CT imaging where two parallel anode samples of Anodes A and B, respectively, were electrolysed for 2000 s, then one was pulled out of the furnace with current still on (hot-pulled) and the other was left in the electrolyte after current had been turned off for 5 mins until pulled out (non-hot-pulled). The thickness of the bathfilm left on the sample surface was determined using the ImageJ software (from U. S. National Institutes of Health) where carbon and electrolyte were distinguished from each other by setting a threshold to the limit value of the density of the two different matters. Contour images of the bathfilm thickness was also produced.

Results and Discussion

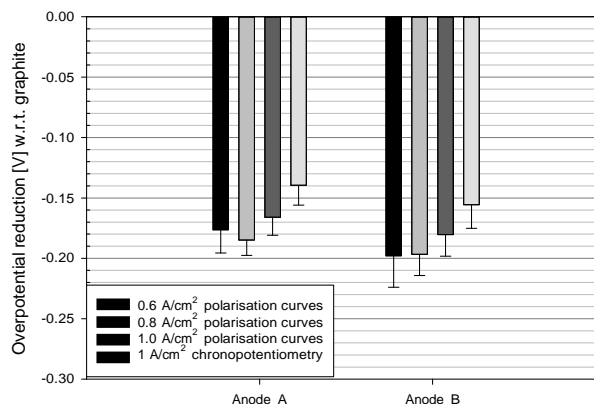


Figure 1: Overpotential reduction for Anode A and Anode B w.r.t. graphite reference at three different current densities (0.6, 0.8 and 1.0 A/cm²) obtained by CV curves and by CP at 1.0 A/cm².

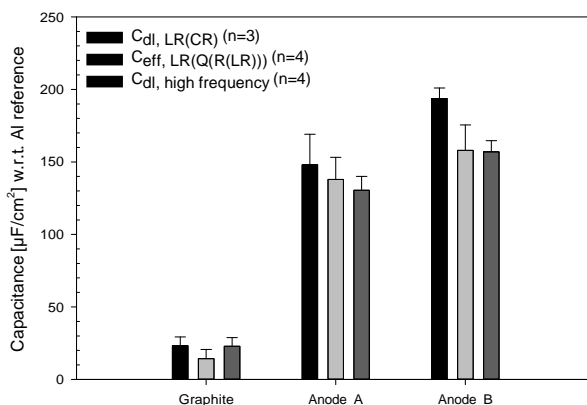


Figure 2: Capacitance for Graphite, Anodes A and Anode B obtained by running electrical impedance spectroscopy at 1.5 V (non-IR corrected).

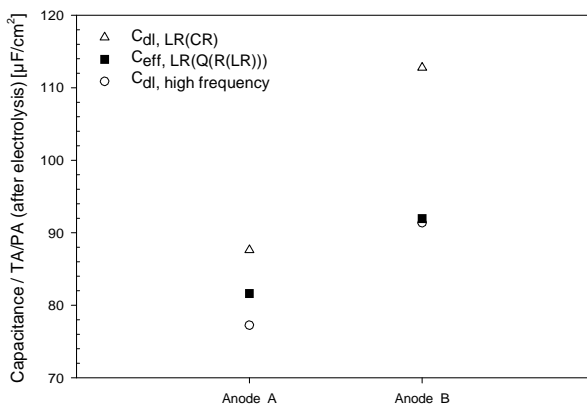


Figure 3: Surface area normalised double layer capacitance.

Figure 1 shows the IR corrected potentials corresponding to 0.6 A/cm^2 , 0.8 A/cm^2 and 1.0 A/cm^2 extracted from CV curves and CP results at 1.0 A/cm^2 . The potential response was recorded with respect to Al reference, furthermore normalised with respect to graphite in order to compensate for some shifts in potential between duplicate runs with new reference electrodes. In general it can be seen that the purely isotropic coke based anode (Anode B), has a slightly lower reaction overpotential (η'_r) of about 15-20 mV, compared with Anode A, at all current densities and independent of measuring technique. This is in accordance with that found and reported elsewhere [3], [4].

Figure 2 shows the capacitance for Graphite, Anode A and Anode B, extracted using three different methods, as described previously. For all three methods it is clear that Graphite has a very low capacitance at around $20 \mu\text{F/cm}^2$ due to its non-porous and almost polished-like surface structure. The industrial anodes show higher capacitance where Anode A have values between $130\text{-}150 \mu\text{F/cm}^2$ and Anode B have values between $155\text{-}195 \mu\text{F/cm}^2$, depending on how the capacitance was extracted from the raw data. The Graphite values are somewhat lower than what Thonstad described [7], but this is probably due to the graphite materials used in the present work being non-identical to Thonstad's, as well as different instruments recording these spectras. Also, the industrial coke anodes are within the lower range to that Thonstad found for his baked carbon even though these materials are certainly not identical or even comparable to each other due to the quality shift in cokes available now, and then.

Confocal microscopy was used in order to determine the real surface area of the anode surfaces including all voids and pores, and this value was reported as true area over projected geographical area (TA/PA). It was found that Anode B had a slightly higher (TA/PA) than Anode A. These area values were then used to determine if the higher capacitance for Anode B compared with Anode A, was merely due to increased surface area of Anode B, the $C_{dl,highfreq.}$ was normalised in terms of true area on the anode as seen in Figure 3. The non-constant value for the surface area normalised $C_{dl,highfreq.}$ indicates that Anode B has a higher electrochemical reactivity than Anode A. It was also shown in [10] that pores had to be very large and of a concave form in order to be filled with electrolyte, with the conclusion that a surface area

including all pores and voids are not necessarily equal to the electrochemical active surface area.

Figure 4 shows measured weight corrected for theoretical weight ($m_m - m_t$) when taking buoyancy into consideration and calculated wetting angle for Graphite, Anode A and Anode B using the immersion-emersion technique as described in [9], [11]. Before polarisation, the wetting difference between Anode A and Anode B is not so pronounced while Graphite shows the highest wetting angle. After polarisation, the wetting changes noticeably. For all anodes tested the wetting towards the electrolyte increases, but the shift is most prominent for Anode B, changing from a wetting angle of about 140° to nearly 90° . This change is highly relevant for the electrochemical reactivity of the anode, and is contrary with the finding in [9] where no difference between wetting angle before and after polarisation during immersion was found. Better wetting between anode and electrolyte means better efficiency of the anode in the potrooms.

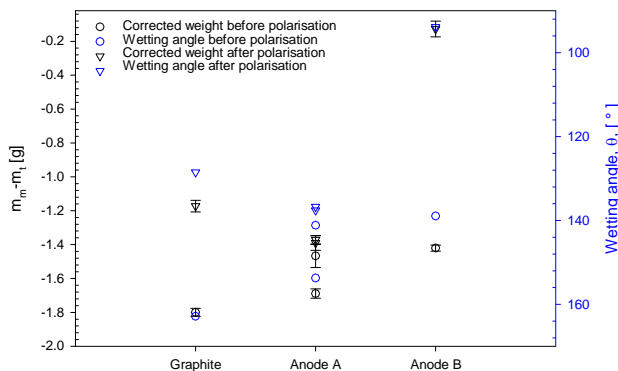


Figure 4: Corrected weight (black) and wetting angle (blue) before (circles) and after (triangles) polarisation.

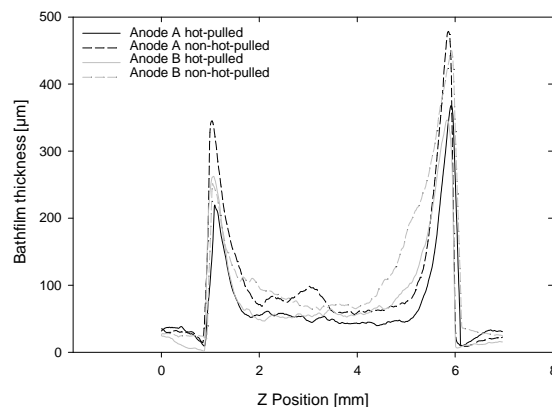
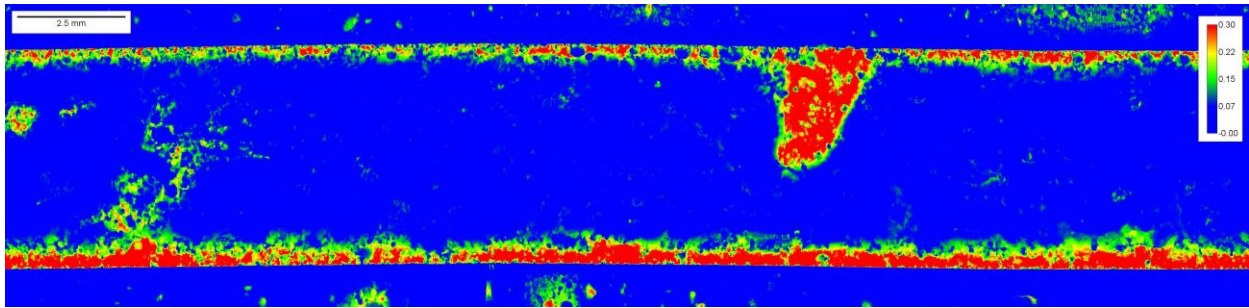
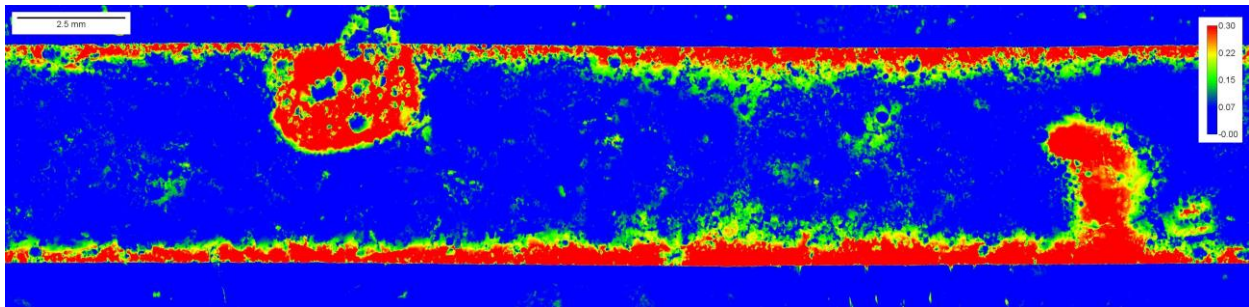


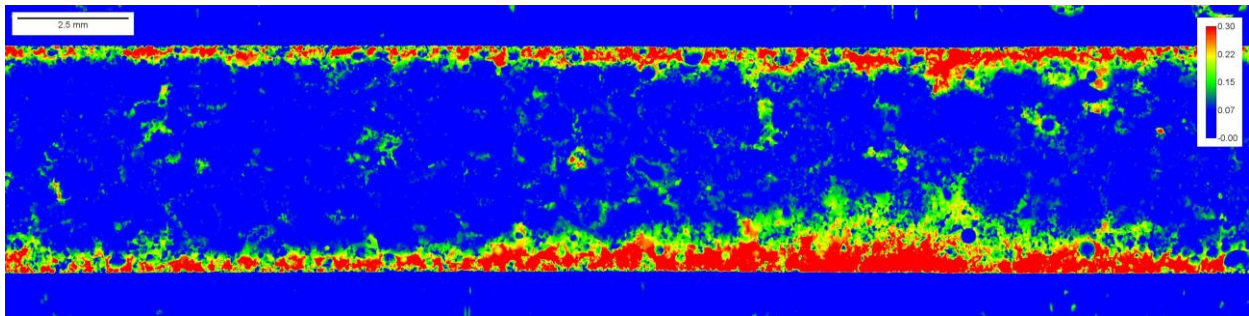
Figure 5: Bathfilm determined by CT scanning of hot-pulled and non-hot-pulled samples.



(a)



(b)



(c)

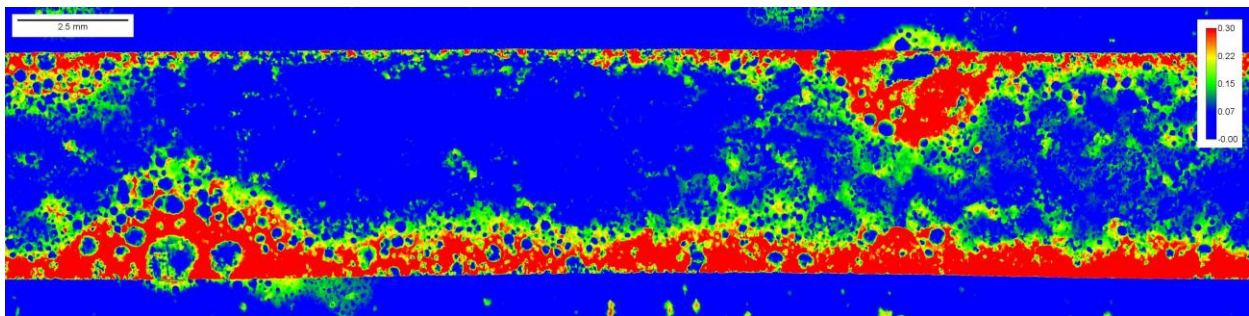


Figure 6: Contour plots of bathfilm obtained by CT. (a) Anode A hot-pulled, (b) Anode A non-hot-pulled, (c) Anode B hot-pulled and (d) Anode B non-hot-pulled.

Wetting behaviour of anode:electrolyte was also investigated by polarising the anodes at 1.0 A/cm², then either hot-pulling or not-hot-pulling. Then the anodes were investigated using CT and extracting the bathfilm thickness on the anode surfaces. Figure 5 shows the bathfilm thickness for Anode A and Anode B, both hot-pulled and non-hot-pulled. Anode B has a slightly thicker bathfilm both during hot-pulling and during non-hot-pulling compared with Anode A, supporting better wetting between Anode B and electrolyte after polarisation compared with Anode A (cf. 4). An edge effect is seen where the bathfilm is thicker towards both ends of the vertical anode sample, but thickest at the bottom (to the right in Z position). This makes sense due to to gravitational forces. Figure 6 shows the corresponding contour images of the bathfilm thickness. Blue areas have thinner bathfilm, while red areas have thicker bathfilm. For Anode A, the large red areas are due to “bubble” coke that protrude out from the matrix. This was also seen in the CT work that was performed in [10]. During hot-pulling CO₂ gas bubbles will keep some of the electrolyte off the anode surface, and this is a likely explanation to why the hot-pulled anodes have a thinner bathfilm than the non-hot-pulled anodes. This work also supports the beneficial effects of hot-pulling anodes while changing anodes in the potroom as hotpulling will require less cleaning of butts.

Conclusion

Isotropic coke anodes showed both higher electrochemical reactivity in terms of lower overpotential, higher capacitance and better wetting properties towards the electrolyte compared with anode produced from anisotropic coke.

Acknowledgement

This work was funded by The Norwegian Research Council and Hydro Aluminium AS through the research project Hal Ultra Performance. A great thank you is sent to Aksel Alstad, Cristian Torres, Ole Tore Buset and Julian Tolchard.

References

[1] L. Edwards, M. Robinette, R. Love, A. Ross, M. McClung, R. Roush, and W. Morgan, “Use of shot coke as an anode raw material,” *Light Metals*, pp. 985–990, 2009.

[2] L. Edwards, N. Backhouse, H. Darmstadt, and

M.-J. Dion, “Evolution of anode grade coke quality,” *Light Metals*, pp. 1207–1212, 2012.

[3] R. Thorne, C. Sommerseth, A. Svensson, E. Sandnes, L. Lossius, H. Linga, and A. Ratvik, “Understanding anode overpotential,” *Light Metals*, pp. 1213–1217, 2014.

[4] R. Thorne, C. Sommerseth, A. Ratvik, S. Rørvik, E. Sandnes, L. Lossius, H. Linga, and A. Svensson, “Correlation between Coke Type, Microstructure and Anodic Reaction Overpotential in Aluminium Electrolysis,” *J. Electrochem. Soc.*, pp. E1–E11, 2015.

[5] R. Thorne, C. Sommerseth, A. Ratvik, S. Rørvik, E. Sandnes, L. Lossius, H. Linga, and A. Svensson, “Bubble Evolution and Anode Surface Properties in Aluminium Electrolysis,” *J. Electrochem. Soc.*, pp. E104–E114, 2015.

[6] J. Thonstad, P. Fellner, G. Haarberg, J. Hives, H. Kvannd, and . Sterten, *Aluminium Electrolysis*. Aluminium-Verlag, 3rd ed., 2001.

[7] J. Thonstad, “The Electrode Reaction on the C, CO₂ Electrode in Cryolite-Alumina Melts-II. Impedance Measurements,” *Electrochimica Acta*, pp. 1581–1595, 1970.

[8] S. Jarek and J. Thonstad, “Double-layer capacitance and polarization potential of baked carbon anodes in cryolite-alumina melts,” *J. Appl. Electrochem.*, pp. 1203–1212, 1987.

[9] A. Solheim, H. Gudbrandsen, A. Martinez, K. Einarsrud, and I. Eick, “Wetting between carbon and cryolitic melts. Part II: Effect of bath properties and polarisation,” *Light Metals*, pp. 671–676, 2015.

[10] C. Sommerseth, R. Thorne, S. Rørvik, E. Sandnes, A. Ratvik, L. Lossius, H. Linga, and A. Svensson, “Spatial methods for characterising carbon anodes for aluminium production,” *Light Metals*, pp. 671–676, 2015.

[11] A. Martinez, O. Paulsen, A. Solheim, H. Gudbrandsen, and I. Eick, “Wetting between carbon and cryolitic melts. Part I: Theory and equipment,” *Light Metals*, pp. 665–670, 2015.

[12] M. Orazem and B. Tribollet, *Electrochemical Impedance Spectroscopy*. Wiley, 1st ed., 2008.